

Modeling the damage evolution in compressed polymer bonded explosives based on computed microtomography images

Rui Liu^{*†}, Ming Li^{*}, Jingming Li^{*}, and Xue Zheng^{*}

^{*}Institute of Chemical Materials, China Academy of Engineering Physics,
Mian shan Road No. 64, You xian District, Mianyang, Sichuan Province, 621900, CHINA
Phone : +0086-0816-2490041

[†]Corresponding address : liurui.imech@gmail.com

Received : August 22, 2012 Accepted : November 1, 2012

Abstract

The evolution of the damage in polymer bonded explosives (PBXs) caused by stepwise compression is studied and x-ray computed microtomography (CT) is applied to investigate microstructures in PBXs. By digital images processing on CT images, the low density and high density regions of interior of PBXs are distinguished. The characteristics of damage are identified in the low density regions. Therefore, the evolution of the damage with the uniaxial compressive process of PBXs is presented by analyzing the change of the low density regions. Meanwhile, correlating CT images with the change of the Young's modulus provides insight into detailed mechanics of the fracture process. The results show that three stages on evolution of the damage are clarified. In the short elastic stage, damage is restricted. As the compressive stress increases, new damage appears and the change of damage is fluctuated. When compressive stress is close to fracture stress, damage increases and develops to form cracks. The three-stage failure model is well matched with experimental data and reveals the relation between the evolution process of damage and the nonlinear mechanics response.

Keywords : material mechanics, polymer bonded explosives, damage evolution, x-ray computed tomography, uniaxial compressive experiment

1. Introduction

High explosives such as polymer bonded explosives (PBXs) are highly particle filled composite materials comprised of crystals of explosives and polymer binders. The mechanical properties of crystals and polymer binders are very different from each other in modulus and strength¹⁾. When they are mixed and pressed to form PBXs, mechanical properties^{2), 3)} of PBXs become more complex to understand. Because a number of studies show that damage and cracks can influence the process of ignition, detonation and so on^{4), 5)}. Thus study of the mechanical properties and failure mechanisms of PBXs is of great importance in the design of compositions, life prediction and safety evaluation of PBXs⁶⁾. In this work, the evolution of damage and nonlinear mechanics response is widely discussed^{7), 8)}.

To understand the mechanical response of PBXs, different types of mechanical testings, such as uniaxial tension, compression, cyclic loading, creep (compression and tension), Brazilian test, Hopkinson bar and so on^{9), 10)}, have been conducted. By these mechanical testings, the process of fracture of material is quantified by measure of stress and strain, by which the macroscopical physical parameters can be obtained. The macroscopical parameters cannot describe the relation between the details of the whole field of physical parameters and the process of fracture. High-resolution non-contact optical technique and digital correlation technique¹¹⁾⁻¹⁴⁾ have been applied in Brazilian test and three-point flexural bend fracture tests with pre-cracks configuration. The growth and movement of pre-cracks is measured successfully. But it still doesn't provide data on damage in the form of

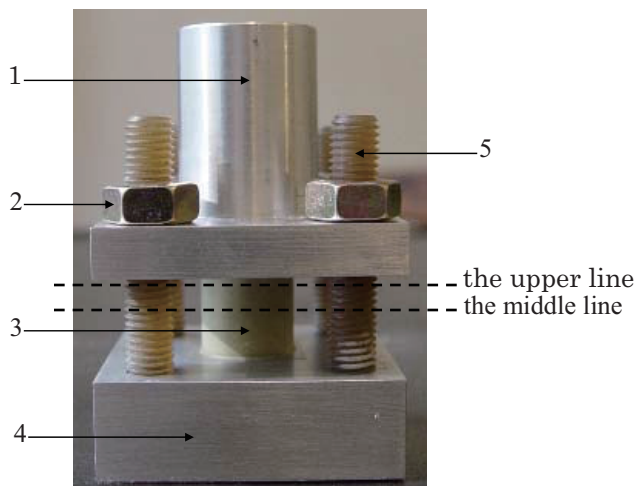
microcracks, debonding, void formation and the growth of existing voids in PBXs' interior. Non-destructive testing techniques, such as Ultra-small angle x-ray scattering, ultra-small angle neutron scattering, x-ray computed microtomography (CT)^{15, 16} and so on, have been developed to investigate voids from a few nanometers to a few micrometers successfully.

In this paper, CT is applied to observe PBXs' interior microstructures subjected to compressive stress. According to CT imaging principle, the low and high density regions can be distinguished. The low density regions contain information of damage. The change of damage in PBXs, which is uniaxially stepwise compressed, is well investigated. By digital images processing on CT images, the characteristics of the change of the damage are presented. The failure mechanism of PBXs under quasi-static compress is analyzed. The results show that three stages on evolution of the damage are clarified and it is well matched with experimental data and nonlinear mechanics response.

2. Experiments

Pressed octahydro-1,3,5,7-tetranitro-1,3,5,7-tetrazocine (HMX) -based PBX1 is used in the experiments. The specimen's diameter is 20 mm and the height 20 mm. The compression rate is 0.5 mm min⁻¹. It is considered as quasi-static uniaxial compress process. The parameters of X-ray CT are magnification 9.09 and x-ray voltage 130 V.

The whole experiment process goes through two steps. First the quasi-static uniaxial compress test is conducted on the specimen. Second it is checked by CT. To avoid damage closing up after upload, as Figure 1 shows, a special experimental setup is designed and the specimen is placed between a press end and a press base. The press end moves along the orientation of compression. When the compressive stress increases to the given value, the press end stop moving and the location of the press end is fixed by nuts. By this method, damage is frozen within the PBXs specimen. The compressive stress is stepwise increase by 0,5 MPa, 10 MPa, 15 MPa, 20 MPa, 25 MPa, 30



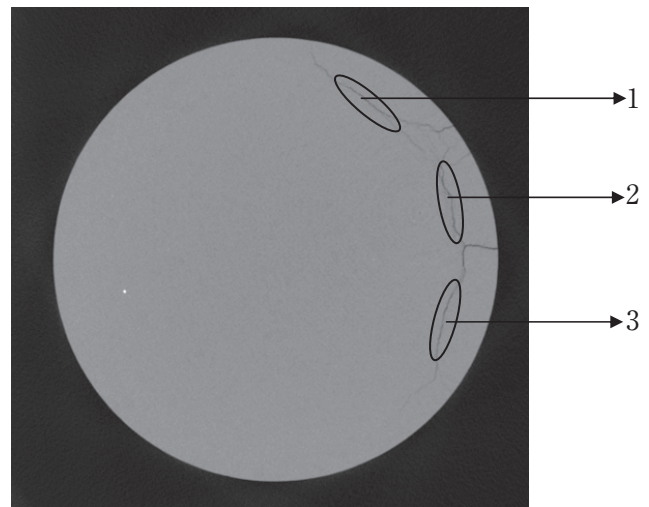
1—the press end, 2—the nut, 3—the specimen, 4—the press base, 5—the orientation screw.
Figure 1 The experimental setup.

MPa respectively. After every step, the interior microstructures of the cross section at the upper line and middle line are observed by CT.

3. Results and discussion

The typical CT images are obtained as shown in Figure 2. Tomographic slices are reconstructed by attenuation of x-rays through the specimen. It is described by $I = I_0 e^{-\mu x}$ where I is the x-ray intensity, x is the distance of the unit which x-ray goes through and μ is an attenuation coefficient, which is depend on the material and the density. Therefore, the dark region of PBXs' interior in the cross section is the low density part, which contains cracks and damage.

According to imaging principle, a high pixel value represents a high density and a low pixel value represents a low density. In Figure 3, the vertical coordinate represents that the number of elements is cumulated in the whole PBXs' interior when the pixel value is higher than the given pixel value. The statistic distribution of the pixel value is obtained. When the given pixel value is above some value, the number rapidly decreases. So there exists a threshold value. It is because materials' density is far above voids' density and the voids are out of statistic. So the inflexion can distinguish the high density part and



1, 2, 3—the dark region.
Figure 2 The typical CT image.

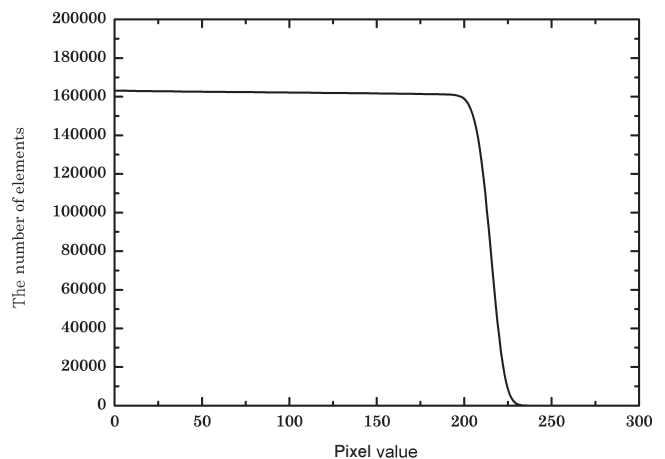
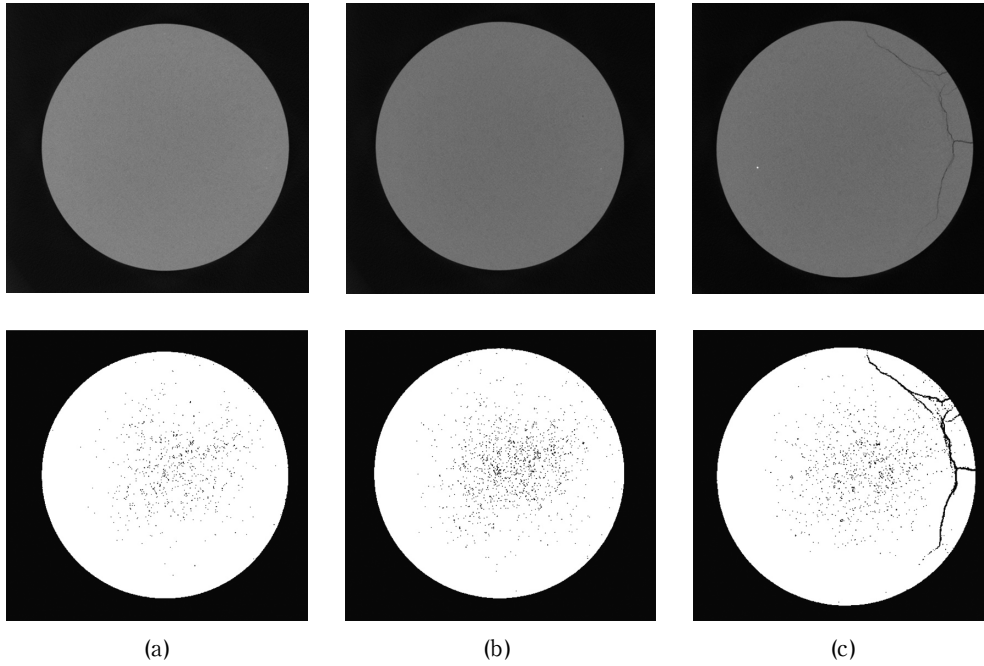


Figure 3 The statistic distribution of pixel value.



On the condition of stress : (a) 15 MPa (b) 25 MPa (c) 30 MPa.
Figure 4 The CT images of interior at the upper line and the binary images.

low density part.

By confirming the inflexion of every CT image, the low density region is obtained. If the pixel value is not lower than the inflexion i , where i is the pixel value, is equal to 1. Otherwise i is equal to 0, where is the low density region. The binary images, which are displayed in Figure 4, are transformed from the CT images.

Figure 5 shows that the low density region of interior at the upper line and the middle line changes in three different processes as the stress increases. In initial stage, the proportion apparently decreases. This process represents part of initial damage is closed up. As the specimen is compressed more, the proportion fluctuates. New damage appears. At the same time, part of damage is also closed up. Until the pressure reaches some value, the proportion rapidly increases. Damage develops to form cracks.

The evolution of damage and the formation of cracks bring about the change of the Young's modulus. The

Young's modulus is defined that $E_{\epsilon=\epsilon_1} = (d\sigma/d\epsilon)_{\epsilon=\epsilon_1}$, where σ is stress and ϵ is strain. As the experimental data in Figure 6 show, after a short elastic stage, the trend of the change E have two states. Therefore, it can be defined as follows :

$$d\sigma/d\epsilon = \begin{cases} A & 0 < \epsilon < \epsilon_0 \\ B\epsilon^{n_1} & \epsilon_0 < \epsilon < \epsilon_1 \\ C\epsilon^{n_2} & \epsilon_1 < \epsilon < \epsilon_2 \end{cases} \quad (1)$$

According to the experimental data of the uniaxial compress test, the parameters in the formula (1) are determinate : $A = 10.64$ GPa, $B = 381.6$ MPa, $n_1 = -0.479$, $C = 22.697$ KPa, $n_2 = -2.2316$.

The stress-strain relation (2) is obtained by integrating the formula (1). The integral constant is confirmed by proceeding the experimental data in the optimization. As Figure 7 shows, the formula (2) matches well with the experimental data. The strain critical value, where the curves intersect between the two connected areas, is

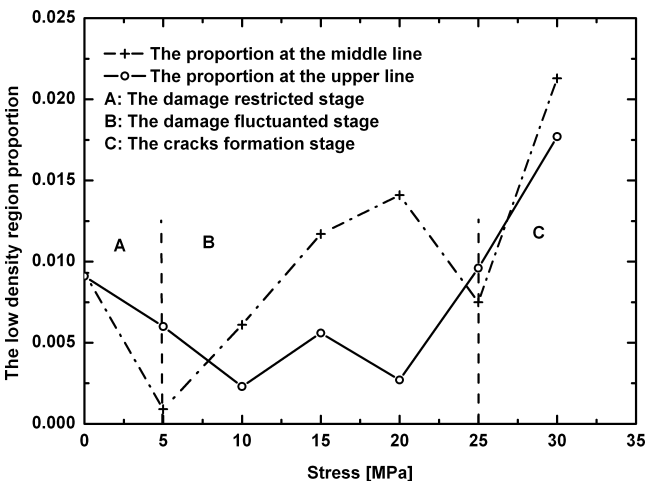


Figure 5 The low density region proportion with the change of the pressure.

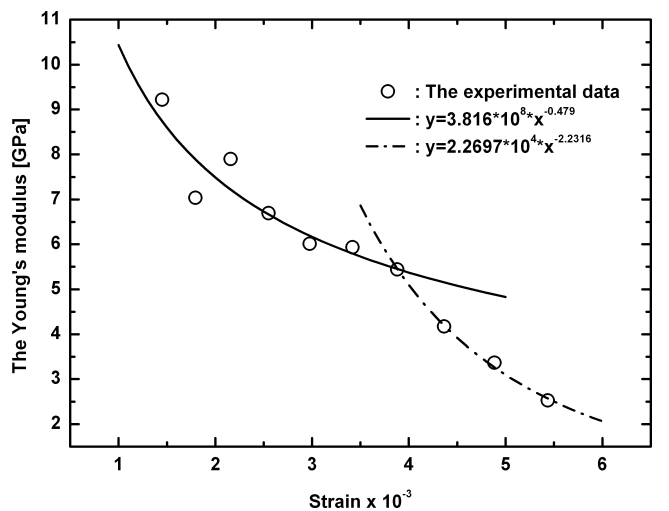


Figure 6 The Young's modulus-strain curve.

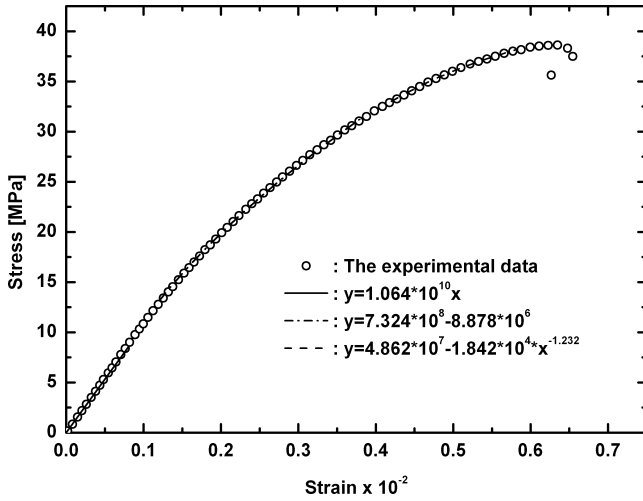


Figure 7 The stress–strain curve.

calculated by the consecutive condition of the stress-strain equations. So ε_0 , ε_1 is solved by the formula (2): $\varepsilon_0 = 5.7 \times 10^{-4}$, $\varepsilon_1 = 3.89 \times 10^{-3}$ and σ_0 , σ_1 is calculated: 6.06 MPa, 31.78 MPa independently.

$$\sigma = \begin{cases} 1.064 \times 10^{10} \varepsilon & 0 < \varepsilon < \varepsilon_0 \\ 7.324 \times 10^8 \varepsilon^{0.521} - 8.878 \times 10^6 & \varepsilon_0 < \varepsilon < \varepsilon_1 \\ 4.862 \times 10^7 - 1.842 \times 10^4 \varepsilon^{-1.232} & \varepsilon_1 < \varepsilon < \varepsilon_2 \end{cases} \quad (2)$$

The evolution of the damage as the CT images show is consistent with the change of the Young's modulus. That is the evolution of damage brings about the nonlinear mechanics response. In fact, the low density region in PBXs interior microstructures contains many tiny air bubbles. So in the process of uniaxial compression air is compressed. Meanwhile the process is considered to be isothermal on the condition of the quasi-static compression. Due to the lower air pressure of voids in the compressive initial stage, the change of the air volume $\Delta V/V = \Delta P/P$ is quantitatively equal to 10. Explosive crystals' Young's modulus is quantitatively 10 GPa and polymer binders' Young's modulus is quantitatively higher than 10 MPa. So voids are more easily compressed than explosive crystals and polymer binders. When the compress stress is lower, it is in the elastic stage that material and voids as the whole are compressed to density. The initial voids include the microcracks which are formed in the process of producing the PBXs specimen. As microcracks are closed up, the surfaces operate each other. The compress stress continuously increases. It makes the air pressure rise and the voids become more difficulty compressed than the initial stage. Meanwhile, the air pressure acts on explosive crystals and polymer binders. Therefore, new microcracks appear. During this stage, part of voids are still closed up. The appearance and close of voids are arbitrary because of randomness of the locations and dimensions of initial voids and so on. The number of damage presents fluctuates. But in macroscopical opinion, the decrease rate of the Young's modulus is regular. When the stress is higher than some value, the damage is connected to form macrocracks. It develops rapidly and makes capability of PBXs' resisting

compressed weak. So the Young's modulus rapidly decreases.

4. Conclusions

Based on CT technology, the information of damage in PBXs' interior is obtained. Evolution of damage is well statistic according to the threshold value by proceeding CT images. Under the quasi-static stepwise compress condition it is introduced into the three-stage failure model for describing the evolution of the damage. In the elastic stage, the initial damage is closed up. It results from that voids are more easily compressed than explosive crystals and polymer binders. As the compress stress increases, PBXs show the properties of plasticity. A small number of new microcracks in crystals and polymer binders appear. During this stage, the number of damage fluctuates. When compress stress continuously enhances, microcracks are connected each other or enlarged. The damage forms cracks so that PBXs are in the failure. The three-stage failure model is supported by the analysis of the Young's modulus on the deformation theory. The law of the change of the Young's modulus has also three steps. The joint value of every stage is approximately equal between the CT results and the results of the Young's modulus. So the three-stage failure model is well matched with experimental data and reveals the relation between the evolution process of damage and the nonlinear mechanics response.

Acknowledgement : The authors are grateful to Professor Maoping Wen, assistant researcher Bin Dai and assistant professor Cunfeng Yang for their effort and support in conducting the experiments.

The work is supported by National Natural Science Foundation (No. 11076032) and National Natural Science Foundation (No. 10832003).

References

- 1) Biswajit Banerjee, Micromechanics–Based Prediction of Thermoelastic Properties of High Energy Materials, PhD thesis, The University of Utah (2002).
- 2) Gert Scholtes, Richard Bouma, Frans Peter Weterings and Albert van der Steen, Proceedings of the 12th international symposium detonation, 121–130, The Netherlands (2002).
- 3) Rae PJ, Quasistatic Studies of the Deformation, Strength and Failure of Polymer–Bonded Explosives, PhD Thesis, The University of Cambridge (2000).
- 4) Steven K. Chidester, Kevin S. Vandersall, Craig M. Tarver, Frank Garcia and Darla Thompson, Proceedings of the 14th international detonation, 921–931, Lawrence Livermore National Laboratory, U.S.A. (2010).
- 5) Bennett JG, Haberman KS, Johnson J N and Asay B W. J. Mech Phys Solids 35, 2303–2322 (1998).
- 6) Stephan R. Bilyk and Michael J. Scheidler, Proceedings of the 13th international symposium detonation, 1286–1296, U. S. Army Research Laboratory, U.S.A. (2006).
- 7) Wu Yanqing and Huang Fenglei, J SCIENCE CHINA Physics, Mechanics & Astronomy, 53, 218–226 (2010).
- 8) Chen Pengwan, Huang Fenglei, and Ding Yansheng, Journal of Beijing Institute of Technology, 13, 43–47 (2004).

- 9) Cheng Liu and Richard Browning, Proceedings of the 12th international symposium detonation, 311–316, Los Alamos National Laboratory, U.S.A. (2002).
- 10) Viet Dung Le, Michel Gratton, Michaël Caliez, Arnaud Frachon and Didier Picart, *J Mater Sci*, 45, 5802–5813 (2010).
- 11) H. Tan, C. Liu, Y. Huang and P. H. Geubelle, *Journal of the Mechanics and Physics of Solids*, 53, 1892–1917 (2005).
- 12) Bruck HA, McNeill SR, Sutton MA and Peters WH, *J Exp Mech*, 29, 261–267 (1989).
- 13) Philip J. Rae, H. Tim Goldrein, Stewart J. P. Palmer and John E. Field. Proceedings of the 12th international symposium detonation, 44–48, Cavendish Laboratory, U.K (2002).
- 14) M. Li, J. Zhang, C. Y. Xiong, J. Fang, J. M Li and Y. Hao, *Optics and Lasers in Engineering*, 43, 856–868 (2005).
- 15) Trevor M. Willey, Lisa Lauderbach, Franco Gagliardi, B. Cunningham, K. T. Lorenz, J. R. I. Lee, T. van Buuren, R. Call, L. Landt and G. Overturf, Proceedings of the 14th international detonation, 530–538, Lawrence Livermore National Laboratory, U.S.A. (2010).
- 16) Zhang Wei-bin, Huang Hui, Tian Yong, Zong He-hou, Dai Bin and Guan Li-feng, *Chinese Journal of Energetic Materials*, 17, 499–500 (2009).